UMYU Scientifica, Vol. 4 NO. 2, June 2025, Pp 457 – 474
https://doi.org/10.56919/usci.2542.048
ISSN: 2955 – 1145 (print); 2955 – 1153 (online)
A periodical of the Faculty of Natural and Applied Sciences, UMYU, Katsina

ORIGINAL RESEARCH ARTICLE

Synthesis, Characterization and Dyeing Performance of Novel Naphthalimide-Based Monoazo Acid Dyes on Nylon 6.6 Fabrics

Amina Muhammad Mustapha[1]*, Umar Ameuru Salami[2], Abdulraheem Giwa[2] and Eli Danladi[3]
[1]Department of Pure and Applied Chemistry, Faculty of Physical Sciences, Kaduna State University, PMB 2339, Kaduna, Nigeria.
[2]Department of Polymer and Textile Engineering, Faculty of Engineering, Ahmadu Bello University, PMB 1500, Zaria, Nigeria
[3]Department of Physics, Federal University of Health Sciences, PMB 145, Otukpo, Benue State, Nigeria

ABSTRACT
Four new monoazo acid dyes were synthesized on the basis of 1,8-naphthalimide core with H-acid, gamma-acid, J-acid and R-acid as coupling components. FTIR, UV-Vis and mass spectrometry verified their structures. Nylon 6.6 was dyed by the exhaust method, and the fastness was determined according to AATCC standards. The dyes exhibited considerable absorption in the visible region (λmax = 515 - 546 nm) with molar extinction coefficients at about 0.89 x 10^4 to 11.1 x 10^4 $L \cdot mol^{-1} \cdot cm^{-1}$. Wash fastness was rated 3-5, perspiration fastness 3-5, light fastness 4-7, and exhaustion was up to 94%. Colorimetric data showed color tunability from violet-purple to pink-magenta, with a chroma index of up to 37, revealing strong color intensity and stability. These findings indicate that the dyes possess high affinity for the fiber, good stability of shade development, and high stability under textile processing conditions. The study was confined to nylon 6.6 under laboratory conditions, and further work is needed to test its behavior on other polyamides and to assess its environmental performance. Overall, the findings substantiate the potential for naphthalimide-derived azo acid dyestuffs as a versatile class of fiber-selective colorants for synthetic textile applications.

ARTICLE HISTORY
Received April 20, 2025
Accepted June 28, 2025
Published June 30, 2025

KEYWORDS
naphthalimide, monoazo acid dyes, nylon 6.6, fastness properties, colorimetry

INTRODUCTION
Synthetic organic colorants form the basis of the aesthetic and functional performance of thousands of products in many industrial sectors, such as textiles, paper, plastics, leather goods, coatings, cosmetics, and food. Ever since the introduction of the first synthetic dyes in the mid-nineteenth century, their synthetic molecules have largely replaced natural colorants due to their superior performance attributes, palette of colors offered, improvements in fastness properties, and economies of scale realized through chemical synthesis. It is also possible to customize the molecular structure, resulting in the production of dyes with targeted affinities to other substrates and performance profiles (Benkhaya *et al.*, 2020; Al-Tohamy *et al.*, 2022). Amid the vast array of synthetic dyes, the azo group is the most commercially important and most commonly used class of organic dyes. Azo dyes (termed as such by the presence of one or more azo chromophores (-N=N-) connecting aromatic or heteroaromatic groups) make up a significant proportion of the total world dye market, encompassing a significant majority of all the organic dyes produced and used worldwide, estimated at 60-70%. These dyes are usually easy and cheap to synthesize, and the most common method is the diazotization of a primary aromatic amine in an azo coupling reaction, with an electron-rich coupling partner, which can be a phenol, naphthol, or an amine (Christie, 2015). This synthetic flexibility permits the production of a vast structural variety which may be tailored to yield almost any color, including the entire visible spectrum. Moreover, numerous azo dyes have high values of molar extinction coefficient, which is equivalent to high tinctorial power, and moderate to good fastness to light, washing, and perspiration, which implies that azo dyes can be used in a wide variety of demanding applications (El-Sayed *et al.*, 2024).

Azo dyes are grouped by the number of azo groups (monoazo, disazo, trisazo, polyazo) or by application method/substrate affinity, resulting in such groups as acid, basic, direct, disperse, and reactive dyes. This success and synthetic accessibility, which constitute the basis of the dominance of azo dyes, testify to a technologically mature discipline in which common synthetic pathways are highly optimized towards large-scale manufacture (Khanum *et al.*, 2023). The use of unusual, structurally resilient structural motifs or functional groups provides a

Correspondence: Amina Muhammad Mustapha. Department of Pure and Applied Chemistry, Faculty of Physical Sciences, College of Computing, Engineering and Science, Kaduna State University, PMB 2339, Kaduna, Nigeria. ✉ amina.mustapha@kasu.edu.ng.
How to cite: Mustapha, A. M., Ameuru, U. S. Giwa, A. & Danladi, E. (2025). Synthesis, Characterization and Dyeing Performance of Novel Naphthalimide-Based Monoazo Acid Dyes on Nylon 6.6 Fabrics. *UMYU Scientifica*, 4(2), 457 – 474. https://doi.org/10.56919/usci.2542.048

potential direction of the synthesis of the next generation of dyes with specific characteristics. At the same time, mass production and use of synthetic dyes, such as the azo group, present environmental concerns regarding manufacturing and effluent discharge. The potential negative impacts of specific dyes and their by-products on human health, as well as the intensive use of water in traditional dyeing techniques, have led to the development of more environmentally friendly alternatives (Zhang *et al.*, 2024). This involves developing greener dyeing processes (such as supercritical carbon dioxide or natural colourants) and creating dyes with enhanced fixation capabilities, thereby reducing the quantity of residual colourants discharged into wastewater (Elmaaty *et al.*, 2022). As such, the improvement of dye performance, especially its fixation and fastness, is both technically and environmentally desirable.

The 1, 8 - naphthalimide architecture, formally known as Benzo[de]isoquinoline-1, 3 - dione, is a highly special and extremely valuable structural motif in dye and materials chemistry. This bicyclic aromatic ring system has an imide moiety that is fused to naphthalene core (Dai *et al.*, 2025). The naphthalimide derivatives can easily be synthesized through condensation of 1,8-naphthalic anhydride or its substituted counterparts with primary amines (Jeong *et al.*, 2022). In addition to stability, 1,8-naphthalimide derivatives are especially known for their unique photophysical and fluorescence properties, resulting in high fluorescence quantum yields (Sanaullah and Walczak, 2025). The absorption and emission characteristics are highly sensitive to structural modifications, allowing for precise tuning of their optical behavior (Geraghty *et al.*, 2021). Critical role is played by substitution on the naphthalene ring, particularly at C-4 position. Substitution at C-4 with electron-donating groups (e.g. amino or alkoxy groups) generally produces a profound bathochromic shift of the absorption spectrum, and this may shift into the visible spectrum and highly affects the fluorescence emission colour and intensity (Gudeika, 2020).

Nylon 6.6 is a synthetic polymer highly demanded in the fields of textiles and technical materials due to its unique set of characteristics, such as high tensile strength, outstanding abrasion resistance, durability, lightweight, and resilience (Autofab, 2024). Nylon 6.6 is mostly coloured with acid dyes. Such dyes are generally anionic, and contain one or more negatively charged groups, usually sulfonate (SO_3^-) groups, which confer water-solubility, and the requisite affinity to the polyamide substrate (Burkinshaw and Son, 2005). New developments in azo dye synthesis have brought out the prospects of naphthalimide derivatives in the textile industry. As reviewed by Dodangeh *et al.* (2021), Gharanjig *et al.* (2017) originally synthesized monoazo disperse dyes based on N-ester-1,8-naphthalimide for dyeing polyester-cotton blends, which showed good thermal stability and dyeing fastness. This highlights the relevance of the use of naphthalimide-based azo dyes in the improvement of textile performance. Ameuru *et al.* (2018) also proved the industrial value of the naphthalimide derivatives and their use in polyester fabrics dyeing under high-temperature conditions without the addition of a dispersing agent and preserving good fastness characteristics. Al-Majidi and Al-Khuzaie (2019) also prepared new azo compounds bearing a 1,8-naphthalimide group by the condensation of 1,8-naphthalic anhydride with p-phenylenediamine or benzidine. These were also diazotized and condensed with substituted phenols to yield azo products, which can serve as acid-base indicators, demonstrating the chemical versatility of such structures. Reported literature on naphthalimide-based monoazo dyes has so far been confined largely to polyester substrates, where the dyes have performed well in terms of visible absorption but merely satisfactory fastness properties. The structural difference and the dyeing conditions resulted in wash and perspiration fastness between grades 4 and 5 and light fastness between grade 3 and 6 (Pendo *et al.*, 2023). In comparison, there are not many studies on nylon and other polyamides. The limited experiments conducted on naphthalimide-based acid dyes on these substrates exhibit exhaustion values of about 65 - 70% under acidic exhaustion dyeing conditions, wash and perspiration resistance is typically Grade 4, and light fastness is typically grade 3 - 4 (Shaki *et al.*, 2015; Hosseinnezhad *et al.*, 2017). Moreover, colorimetric shade difference on nylon 6.6 has not been reported systematically and comprehensively, leaving a gap in the knowledge of these types of acid dyes' behavior on the polyamide fibers. This deficiency underscores the need for targeted research on the shade tunability and fiber-dye interaction, as well as the fastness performance of such systems under standard test conditions. In this study, four novel naphthalimide-based monoazo acid dyes were synthesized, characterized, and applied to nylon 6.6 in order to evaluate their dyeing behavior, fastness properties, and colorimetric performance.

MATERIALS AND METHODS

All the reagents and solvents for syntheses and analyses were sourced from Sigma-Aldrich and used as supplied without any further purification. The organic materials used for the synthesis of the dyes include Nitroacenaphthene (purity ≥ 98%), 2,4-Dinitroaniline (purity ≥ 98%), 2-amino-4-nitrobenzoic acid (purity ≥ 99%), H-acid (purity ≥ 99%), γ-acid (purity ≥ 98%), J-acid (purity ≥ 98%), R-acid (purity ≥ 99%), and ethanol (purity ≥ 99%), all sourced from Sigma-Aldrich.

Synthesis of 4-nitro-1, 8-naphthalic anhydride

Nitroacenaphthene (0.125 mol, 6.22g) was dissolved in hot acetic acid (62.2 cm^3), and sodium dichromate (39.63 g) was added for 3 hours at 65 – 70 ^oC. The solution was gradually warmed to 98 – 100 ^oC for 30 minutes and refluxed for 5 hours. Hot water (150 cm^3) was used to wash out the contents, followed by cooling and filtering. The solid was washed with dilute HCl and then boiled with 5% Na_2CO_3 (50 cm^3) for 30 minutes and filtered. Acidification of the filtrate was carried out followed by crystals separation and drying for 4 hours at 120 ^oC to yield 4-nitro -1, 8- naphthalic anhydride, which was crystallized

from nitric acid (1.40 g/mL) to produce needle-shaped crystals (Ameuru *et al.*, 2018).

Synthesis of 4-nitro-N-2, 4-dinitrophenyl-1, 8-naphthalimide (A1)

4-nitro-1,8-naphthalic anhydride (2.43 g, 0.02 mol) and 2, 4 – dinitroaniline (2.75 g, 0.03 mol) were suspended in ethanol (51 cm^3) and refluxed for 7 hours under constant stirring. The reaction mixture was allowed to cool, followed by filtration and recrystallization using ethanol. The same method was used to prepare compound A2 using R2 (as shown in Scheme 1).

Synthesis of 4-amino-N-2, 4-dinitrophenyl-1, 8-naphthalimide (B1)

A suspension of 4-nitro-N-2, 4-dinitrophenyl-1, 8-naphthalimide (18 mmol, 2.75 g) and stannous chloride (90 mmol, 8.65 g) in ethanol (30.5 cm^3) was subjected to reflux with conc. Hydrochloric acid (3.8 cm^3) for 1 hour. The reaction mixture was poured into 37.6 cm^3 of water leading to the formation of a precipitate that was filtered off. Recrystallization of the crude product from ethanol afforded brown crystals. The same method was used to prepare compound B2.

Diazotization of 6-amino-2-(2,4-dinitrophenyl)-1*H*-benzo[de]isoquinoline-1,3((2*H*)-dione

Dry sodium nitrite (1.2 mmol, 0.083 g) was added slowly to concentrated H_2SO_4 (98 %, 0.88 cm^3) at below 10 °C. Using a water bath, the temperature of the reaction mixture was elevated to 65 °C to facilitate the dissolution of sodium nitrite. After cooling the solution to 0 – 5 °C, a mixture comprising 8.8 cm^3 of propionic acid and acetic acid (1.5:8.5 v/v) was introduced dropwise with continuous stirring, followed by gradual increase in temperature to 10 – 15 °C. Portion-wise addition of finely ground 4-amino-N-substituted-1, 8-naphthalimide (1.2 mmol, 0.454g) was carried out under continuous stirring for 3 hours. The freshly prepared diazonium salt solution was then employed directly in the coupling reaction.

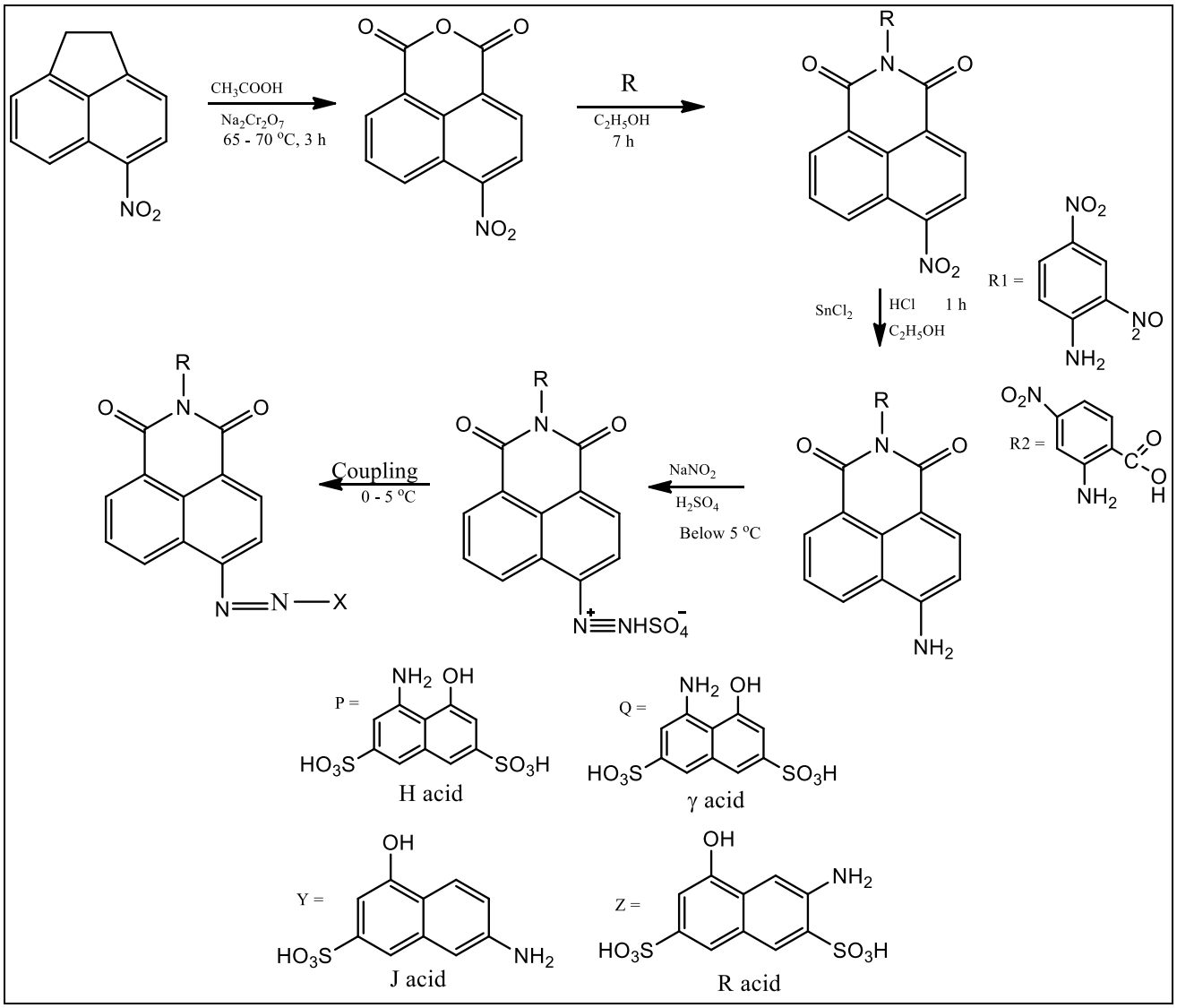

Scheme 1: Synthesis of intermediates and dyes

Where X = P and Q for Dye A and Dye B

X = Y and Z for Dye C and Dye D

Synthesis of acid dyes based on 4-amino-N-substituted-1, 8-naphthalimide intermediate (B1)

The coupling components, 1-naphthol-8-amino-3,6-disulfonic acid (H-acid) (1.2 mmol, 0.383g) for Dye A, 2-amino-8-naphthol-6-sulfonic acid (γ-acid) (1.2 mmol, 0.287g) for Dye B, 2-amino-5-naphthol-7-sulfonic acid (J-acid) (1.2 mmol, 0.287g) for Dye C and 2-amino-8-naphthol-3,6-disulfonic acid (R-acid) (1.2 mmol, 0.383g) for Dye D was each dissolved in 10 % sodium hydroxide solution, followed by the addition of a few drops of acetic acid added at 0 – 5 °C. Dropwise addition of the preformed diazonium solution was carried out over 30 – 40 minutes with constant stirring. The mixture was maintained at 0 – 5 °C and stirred for a further 2 hours. The pH was then adjusted to 4 – 5 with 10 % sodium acetate, followed by an additional hour of stirring. The obtained solid was isolated by filtration, dried and subsequently recrystallized from methanol to give 4-amino-3-((2-(2,4-dinitrophenyl)-1,3-dioxo-2,3-dihydro-1H-benzo[de]isoquinolin-6-yl)diazenyl)-5-hydroxynaphthalene-2,7-disulfonic acid and 6-amino-7-((2-(2,4-dinitrophenyl)-1,3-dioxo-2,3-dihydro-1H-benzo[de]isoquinolin-6-yl)diazenyl)-4-hydroxynaphthalene-2-disulfonic acid. The reaction pathway is depicted in Scheme 1.

Instrumentation and characterization

FTIR spectra were measured on Shimadzu FTIR-84005 spectrometer, in a wavelength range of 4000-400 cm -1 using KBr pellets; polystyrene film standard was used to calibrate the instrument. UV-Vis measurement was performed using a PerkinElmer Lambda 25 spectrophotometer in a 1 cm quartz cuvette with distilled water as the reference, and measurements were taken between 200-800 nm range. GC-MS analyses were also carried out using an Agilent Technologies 7590B GC coupled to a 5977A MSD instrument operated in electron ionization (EI, 70 eV) mode; the instrument was tuned daily with perfluorotributylamine (PFTBA); separations were provided by a fused silica capillary column (HP-5MS, 30 m x 0.25 mm x 0.25 um). Melting points of the synthesized compounds were determined on a Gallenkamp melting point apparatus (model CD10127).

Dyeing Procedure

Dyeing of nylon 6.6 was carried out by the exhaust method using an Ahiba Datacolor IR dyeing machine (Model 2000). Dyebaths were prepared at concentrations of 1%, 3%, and 5% on weight of fabric (owf) using acetic acid–sodium acetate buffer adjusted to pH 4.5. One gram of nylon 6.6 fabric was introduced into a dyebath (liquor ratio 50:1) at 40 °C, raised at 1.5 °C/min to 80 °C, and held for 60 minutes with agitation. The dyed samples were rinsed, squeezed to remove excess liquor, and air-dried. Each dyeing was performed in triplicate (n = 3). The percentage dye exhaustion (%E) was determined from absorbance of the dyebath before (OD_1) and after dyeing (OD_2) at λmax for each dye as shown in equation 1.

$$\%E = \frac{OD1 - OD2}{OD1} \times 100\%$$

Fastness Testing

Fastness properties were assessed using the American Association of Textile Chemists and Colorists (AATCC) standard methods: wash fastness by AATCC 61-2019, perspiration fastness (acidic and alkaline) by AATCC 15-2013, and light fastness by AATCC 16.3-2014. Wash and perspiration tests were conducted using an SDL Atlas Launder-Ometer (Model M231), and light fastness was evaluated using an Atlas Ci3000+ Xenon Weather-Ometer. Each test was repeated three times (n = 3), and ratings were obtained using grayscale.

Colorimetric Analysis Procedure

The dyed nylon 6.6 fabrics were analyzed in colorimetric terms using the CIE model of color space that has become popular in the field of color due to its extensive description of human color perception (CIE, 1931). Firstly, the hexadecimal (HEX) values of the fabrics were used to quantify the fabric color, which was in turn changed to the RGB value through the matplotlib library (Hunt, 2004). The RGB values were next scaled to 0-1 so that they would remain compatible with the color space transformations. The RGB values were then converted to XYZ color space using CIE 1931 XYZ color space using the standard mathematical conversion formula (Cohen *et al.*, 1968), and the XYZ values were then translated into CIE Lab* color coordinates, which is a very common color model being utilized in textile color measurement (Hunt, 2004). The colors were then represented accurately in terms of lightness (L*), green-red (a*), and blue-yellow (b*) axis dimensions. The values of a* and b* were used to compute the chroma (C*) and the hue angle (h°) as shown in equations (2) and (3).

$$\text{Chroma } (C^*) = \sqrt{(a^2 + b^2)} \quad \ldots 2$$

$$\text{Hue angle } (h^\circ) = \tan^{-1}(b^*/a^*) \quad \ldots 3$$

These values provide a detailed understanding of color saturation and hue orientation, which are critical for evaluating color quality and dye performance on the substrate (Westland *et al.*, 2012).

RESULTS AND DISCUSSION

Physical Properties of the Samples

The synthesized samples are coloured crystals with well-defined range of melting points. The physical and spectroscopic properties are depicted in Table 1.

Table 1 summarizes the spectroscopic and physical properties of the synthesized dyes. The melting point of all dyes was high above 300 °C, which implies they were highly stable and impurity-free. Percentage yield between 61.45 (Dye C) and 94.03 (Dye D) was obtained. All synthesized dyes exhibited strong absorption in the visible region, consistent with their observed crystal colors (Table 1). The λ_{max} values ranged from 515 nm (magenta, Dye D) to 546 nm (violet, Dye A), reflecting the influence of

different substituents on the conjugated naphthalimide–azo system. Three dyes (A - C) displayed high molar extinction coefficients (ε_{max} > 1 × 10^4 L mol^{-1} cm^{-1}), indicating strong tinctorial strength, with Dye A recording the highest value (11.1 × 10^4 L mol^{-1} cm^{-1}). In contrast, Dye D exhibited a markedly lower ε_{max} (0.89 × 10^4 L mol^{-1} cm^{-1}), consistent with its weaker resonance stabilization and reduced depth of shade.

Table 1: Physical and spectroscopic characteristics of the synthesized azo acid naphthalimide dyes

Intermediate & Dye code	Molecular formula	Molecular mass ($gmol^{-1}$)	Melting Point (^oC)	Yield (%)	Colour of crystals	H_2O λ max (nm)	ε max in water $x10^4 Lmol^{-1}cm^{-1}$
B1	$C_{18}H_{10}N_4O_6$	378	>300	75.32	Coffee brown	ND	ND
B2	$C_{19}H_{11}N_3O_6$	377	>300	92.03	Light brown	ND	ND
A	$C_{28}H_{16}N_6O_{13}S_2$	708	>300	83.78	Violet	546	11.1
B	$C_{28}H_{15}N_6O_{10}S$	628	>300	65.91	Purple	545	7.4
C	$C_{29}H_{17}N_5O_{10}S$	627	>300	61.45	Purple	533	3.4
D	$C_{27}H_{17}N_5O_{13}S_2$	707	>300	94.03	Magenta	515	0.89

ND – Not determined

Table 2: Structures of the Naphthalimide-based intermediates and acid dyes

Intermediate & Dye code	Name and structure
B1	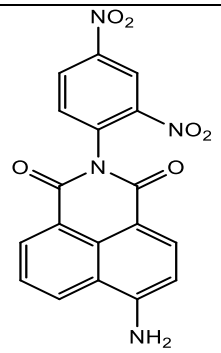 6-amino-2-(2,4-dinitrophenyl)-1H-benzo[de]isoquinolin-1,3(2H)-dione
B2	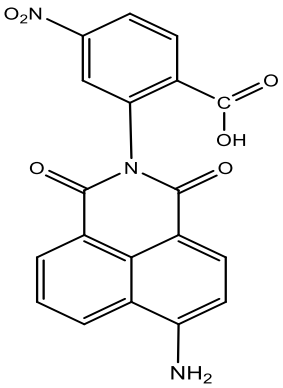 2-(6-amino-1,3-dioxo-1H-benzo[de]isoquinolin-2(3H)-yl)-4-nitrobenzoic acid
A	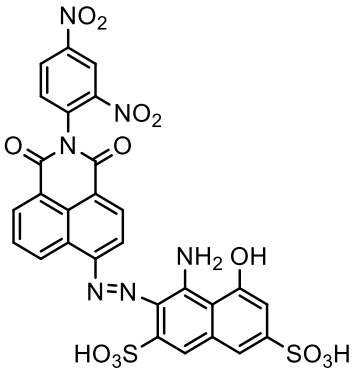 4-amino-3-((2-(2,4-dinitrophenyl)-1,3-dioxo-2,3-dihydro-1H-benzo[de]isoquinolin-6-yl)diazenyl)-5-hydroxynaphthalene-2,7-disulfonic acid

To be continued next page

Table 2 Continued

Intermediate & Dye code	Name and structure
B	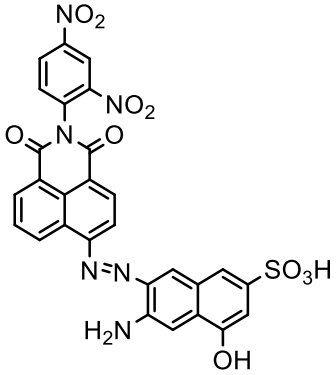 6-amino-7-((2-(2,4-dinitrophenyl)-1,3-dioxo-2,3-dihydro-1H-benzo[de]isoquinolin-6-yl)diazenyl)-4-hydroxynaphthalene-2-disulfonic acid
C	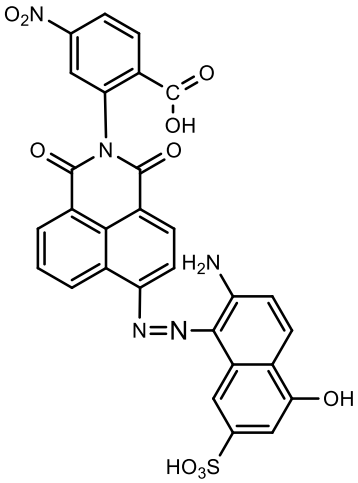 2-(6-((2-amino-5-hydroxy-7-sulfonaphthalen-2-yl)diazenyl)-1,3-dioxo-1H-benzo[de]isoquinolin-2(3H)-yl)-4-nitrobenzoic acid
D	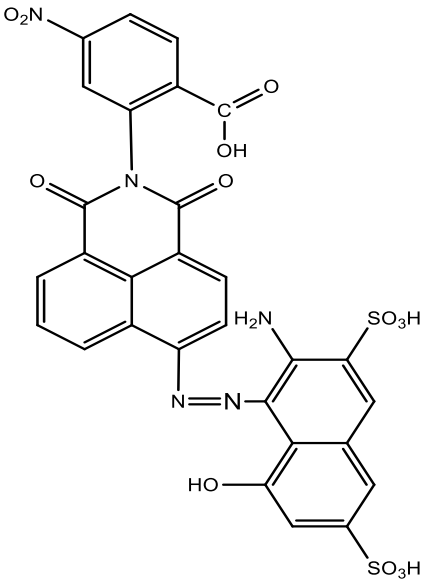 2-(6-((7-amino-1-hydroxy-3,6-disulfonaphthalen-2-yl)diazenyl)-1,3-dioxo-1H-benzo[de]isoquinolin-2(3H)-yl)-4-nitrobenzoic acid

FTIR Spectra of the Synthesized Samples

The FTIR spectra and spectral band assignments of the synthesized monoazo naphthalimide-based acid dyes give an indication of their chemical structure and are presented in Figure 1a, 1b, and Table 3. The presence of the key functional groups for each of the proposed structures was verified from the FTIR spectra of dyes A-D. A single wide absorption band in the region of 3200-3400 cm-1 with

minima at 3391 cm^{-1} (A), 3368 cm^{-1} (B), 3418 cm^{-1} (C), and 3413 cm^{-1} (D) was assigned to overlapping O-H and N-H stretching vibrations. The width of this band reflects the strong hydrogen bonding between sulfonic, hydroxyl, carboxyl, and amino groups, which enhances the solubility and can provide high affinity for dye-fibers in nylon (Papapetros *et al.*, 2023; Mello, 2024). Aromatic C-H stretches were observed slightly above 3000 cm^{-1}, and strong carbonyl absorptions in the range of 1728-1682 cm^{-1} confirmed the imide C=O stretches of the naphthalimide core. Signals for the azo linkage (1511-1528 cm^{-1}) and nitro substituents (1344-1355 cm^{-1}) confirmed the presence of both groups in the dye structures as expected by design.

Table 3: FTIR Data and functional group assignments of the synthesized dyes A, B, C, and D

Functional group	**N-H / O-H**	**C-H**	**C=O**	**C=C**	**N=N**	**NO_2**	**S=O**	**S=O**	**C-H**
Type of vibration (cm^{-1})	Str	Ar. Str	Str	Ar. Str	Str	Str	Sym. Str	Asym. Str	Out-of-plane bending Ar-H
Dye A	3391	3078	1728-1695	1567	1511	1346	1193	1048	898
Dye B	3368	3050	1734-1689	1572	1528	1355	1176	1020	897-717
Dye C	3418	3039	1728-1682	1561	1405	1350	1160	1031	769-721
Dye D	3413	3022	1717-1691	1578	1523	1344	1193	1054	856

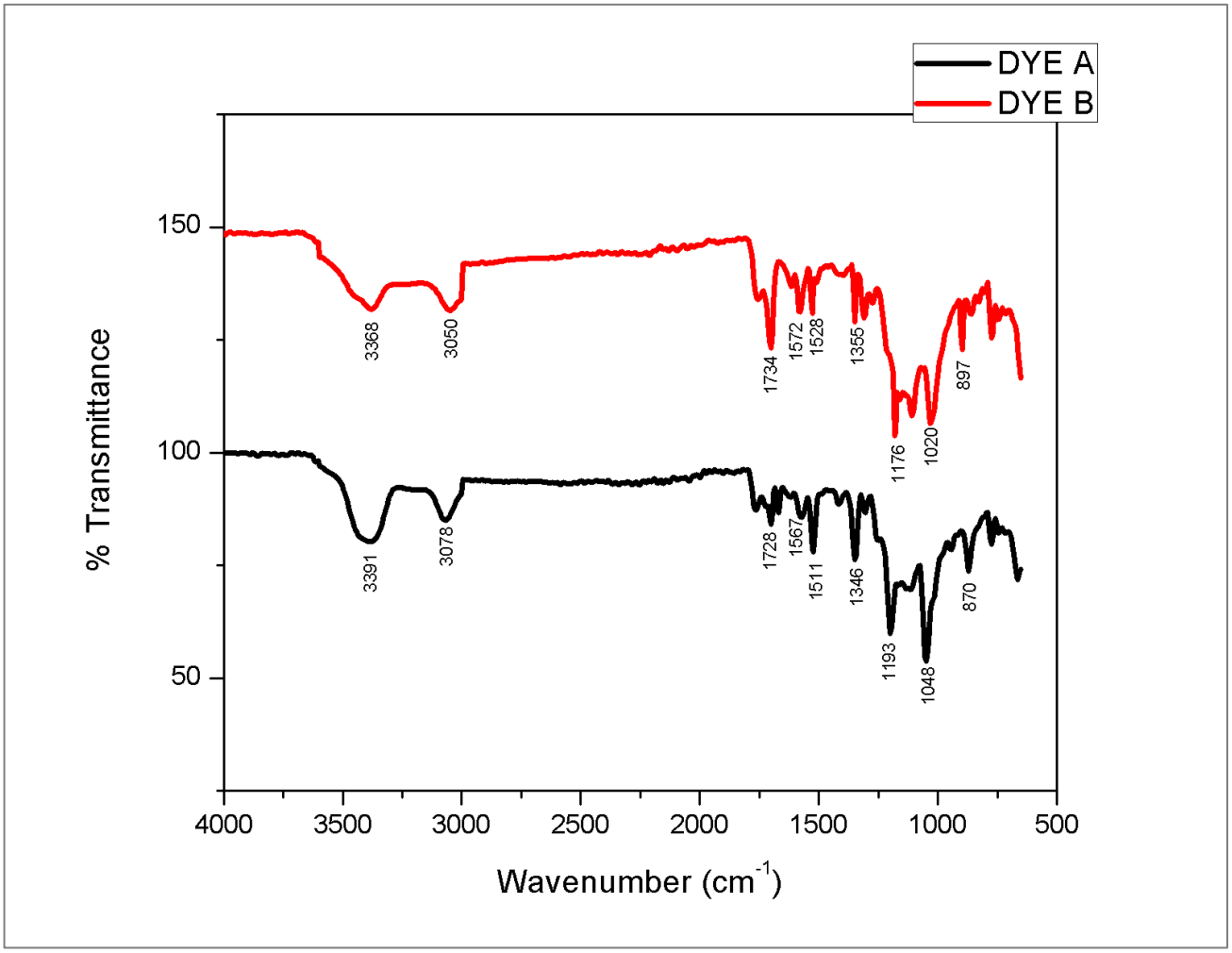

Figure 1a: FTIR spectrum showing the characteristic absorption bands of the synthesized dyes A and B

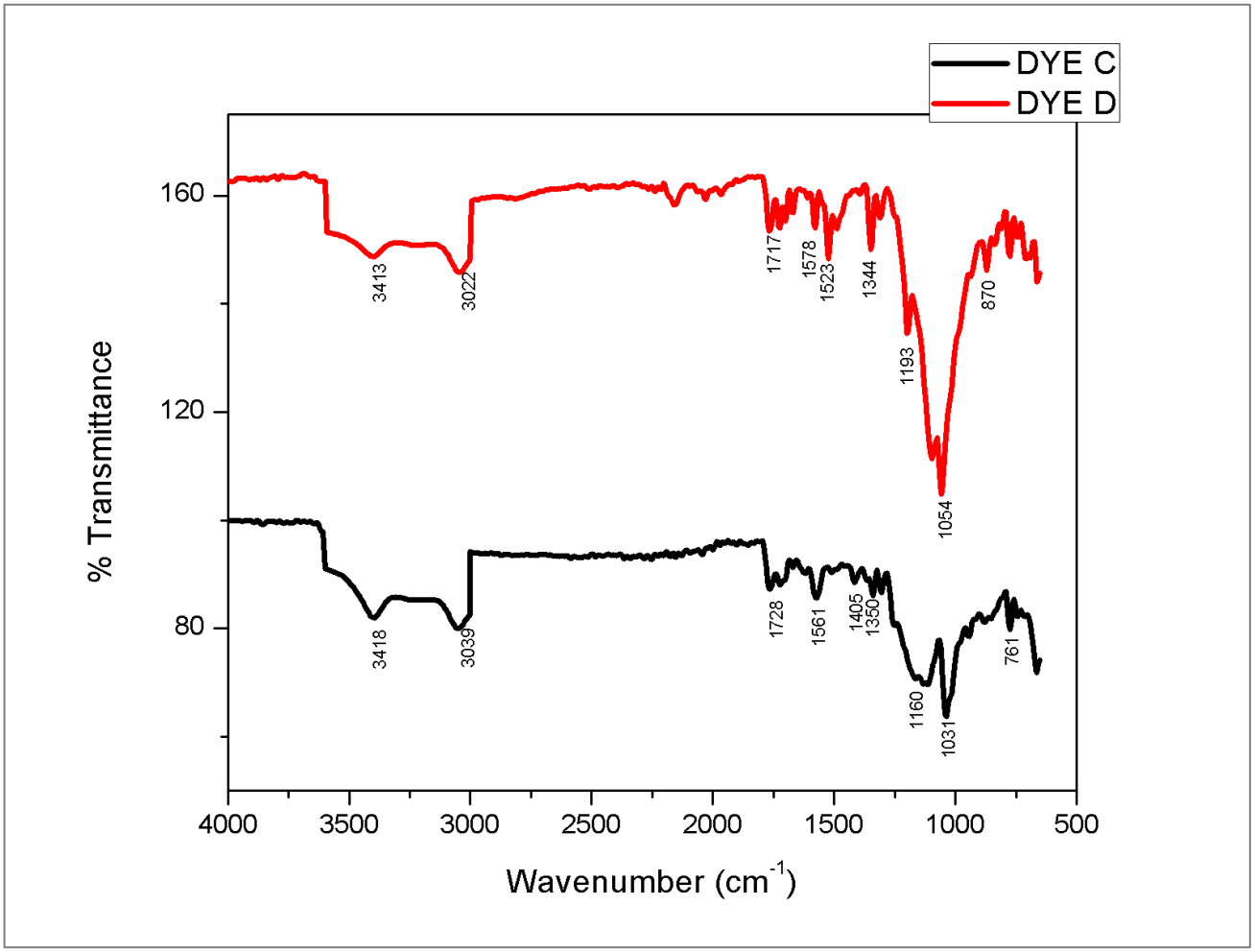

Figure 1b: FTIR spectrum showing the characteristic absorption bands of the synthesized dye C and D

Bands in the regions of 1160-1193 cm^{-1} (symmetric) and 1020-1054 cm^{-1} (asymmetric) were attributed to the sulfonic acid group, with an increase in intensities in Dyes A and D that contain two SO3H substituents. This structural difference is functionally relevant as increased sulfonation contributes to water solubility and ionic bonding to protonated amide functionalities in nylon, which are responsible for the higher uptake and improved fastness (Soleimani-Gorgani and Taylor, 2006; Aspland, 1997). Fingerprint absorption in the range below 1000 cm^{-1}, including out-of-plane bending C-H for aromatic structure as well, confirmed the conservation of the aromatic backbone throughout the series. Together, the results establish the purity of the dyes and report the impact of sulfonation and substituent variations on dye fiber interactions, which provides a sound rational basis for performance optimization and environmentally friendly dyeing in the case of nylon.

Mass spectroscopy of the synthesized monoazo naphthalimide-based acid dyes

The mass spectra of the synthesized dyes (A - D) exhibited fragmentation patterns consistent with their proposed structures. The similarity between all dyes was the presence of the m/z 257 ($C_{14}H_{11}NO_4^+$) characteristic fragment typical of the azo acid motif. Ions of low m/z (55 - 96) tend to be common in all dyes and are likely to be oxygenated or nitrogen-containing cationic species as a result of the cleavage of side chains or heteroatom-rich fragments. Mid-range ions (130 - 200) indicated stable aromatic or heterocyclic units, while larger fragments above m/z 300 reflected intact conjugated naphthalimide-azo segments. Each of these dyes had unique attributes despite these similar characteristics. The presence of the mid-range ions with m/z 135, 199, 224, 281, 327, and 446, as well as larger fragments, 281, 327, and 446, was characteristic of Dye A, and its molecular ion peak at m/z 708 ($C_{28}H_{16}NO_{13}S_2^+$), as expected, confirmed the correct molecular weight. Dye B had clear low-mass fragments at m/z 60 and 82, as well as larger ions at 355 and 515, and a molecular ion at m/z 609, a little lower than the theoretical 628, probably reflecting in-source fragmentation. Dye C produced benzyl-type ions at m/z 91, as well as fragments at 147 and 189 are indicative of nitrogen- and oxygen-substituted aromatics. Larger fragments at 327 and 406 suggested the retention of extended azo-aromatic frameworks, and its molecular ion at m/z 614 was near the calculated 627. Dye D exhibited oxygenated ions at m/z 55, 88, and 96, and other aromatic fragments 159, 186, and high mass ions 331, 401, 501, 574. Its molecular ion at m/z 704 was closely matched to that (707) of the theoretical, a slight difference due to isotopic variation. The mass spectrometric results together established the naphthalimide-azo-sulfonate structure in all of the dyes, and the high-mass ions and molecular ion peaks have indicated the minor structural differences brought by the different substituents.

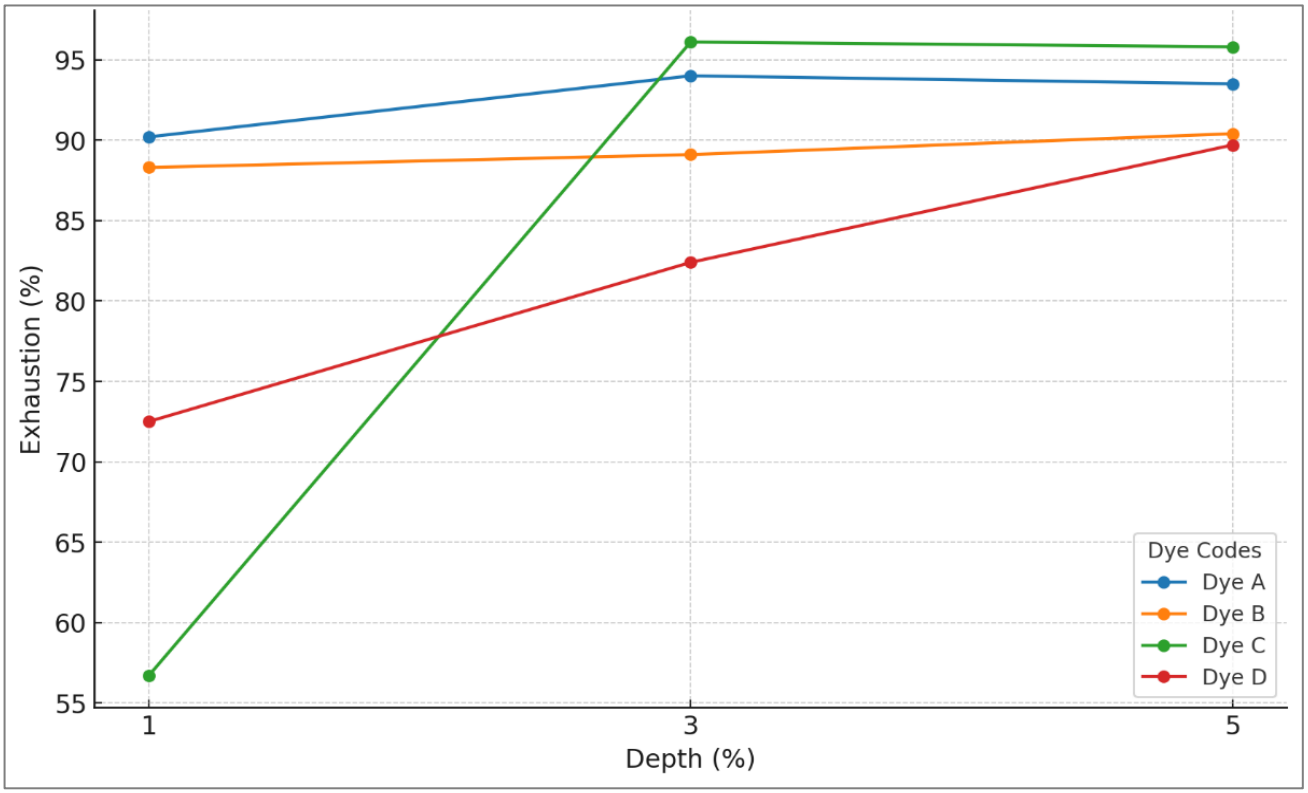

Figure 2: Exhaustion vs depth for the Naphthalimide-based azo acid dyes

Table 5: Exhaustion vs depth for the Naphthalimide-based azo acid dyes

Dye Code	Depth	% Exhaustion (mean ± SD)
Dye A	1%	90.2 ± 1.1
	3%	94.0 ± 0.8
	5%	93.5 ± 1.2
Dye B	1%	88.3 ± 0.9
	3%	89.1 ± 1.0
	5%	90.4 ± 1.3
Dye C	1%	56.7 ± 2.2
	3%	96.1 ± 0.7
	5%	95.8 ± 0.9
Dye D	1%	72.5 ± 1.5
	3%	82.4 ± 1.8
	5%	89.7 ± 1.4

Table 6: Fastness Test for Nylon 6.6

Dye Code	Depth	Color Fastness	Staining	Perspiration (Acid)	Perspiration (Alkaline)	Light Fastness
Dye A	1%	3.00 ± 0.00	4.00 ± 0.00	3.33 ± 0.33	4.00 ± 0.00	5.00 ± 0.00
	3%	3.33 ± 0.33	4.00 ± 0.00	4.00 ± 0.00	4.25 ± 0.25	5.00 ± 0.00
	5%	4.00 ± 0.00	3.00 ± 0.00	4.00 ± 0.00	5.00 ± 0.00	6.00 ± 0.00
Dye B	1%	2.67 ± 0.33	3.00 ± 0.00	3.00 ± 0.00	3.33 ± 0.33	5.00 ± 0.00
	3%	3.00 ± 0.00	3.00 ± 0.00	3.33 ± 0.33	3.67 ± 0.33	5.00 ± 0.00
	5%	3.33 ± 0.33	4.00 ± 0.00	4.33 ± 0.33	5.00 ± 0.00	6.00 ± 0.00
Dye C	1%	4.00 ± 0.00	4.00 ± 0.00	3.00 ± 0.00	3.33 ± 0.33	6.00 ± 0.00
	3%	3.50 ± 0.50	4.00 ± 0.00	3.00 ± 0.00	3.00 ± 0.00	7.00 ± 0.00
	5%	4.50 ± 0.50	4.00 ± 0.00	4.25 ± 0.25	5.00 ± 0.00	7.00 ± 0.00
Dye D	1%	3.50 ± 0.50	3.00 ± 0.00	3.25 ± 0.25	3.50 ± 0.50	4.00 ± 0.00
	3%	4.00 ± 0.00	4.00 ± 0.00	4.00 ± 0.00	4.25 ± 0.25	5.00 ± 0.00
	5%	4.50 ± 0.50	4.00 ± 0.00	4.33 ± 0.33	5.00 ± 0.00	5.00 ± 0.00

Values are expressed as Mean ± SD

Table 7: Colour data and CIE coordinates of the dyes on nylon 6.6

Dyes	Depth	L*	a*	b*	C*	h°	Colour region
Dye A	1%	48.84	29.0	-23.2	37.14	321.7	Purple-violet
	3%	17.41	0.0	-34.0	34.2	270.0	Pure blue
	5%	13.45	7.0	-34.4	35.1	281.5	Blue-violet
Dye B	1%	36.66	1.0	-20.0	20.0	272.9	Blue-purple
	3%	34.98	1.0	-17.6	17.6	273.3	Blue-purple
	5%	20.89	7.5	-25.4	26.6	286.5	Violet
Dye C	1%	64.4	7.5	-14.6	16.4	296.3	Purple
	3%	41.37	11.84	-33.74	35.76	289.3	Blue-violet
	5%	34.9	9.0	-23.8	25.45	290.7	Violet-magenta
Dye D	1%	73.4	5.5	-12.0	13.2	294.9	Purple-pink
	3%	71.0	9.0	-8.6	12.4	316.7	Magenta-purple
	5%	63.5	21.5	-3.5	21.8	350.8	Pink-magenta

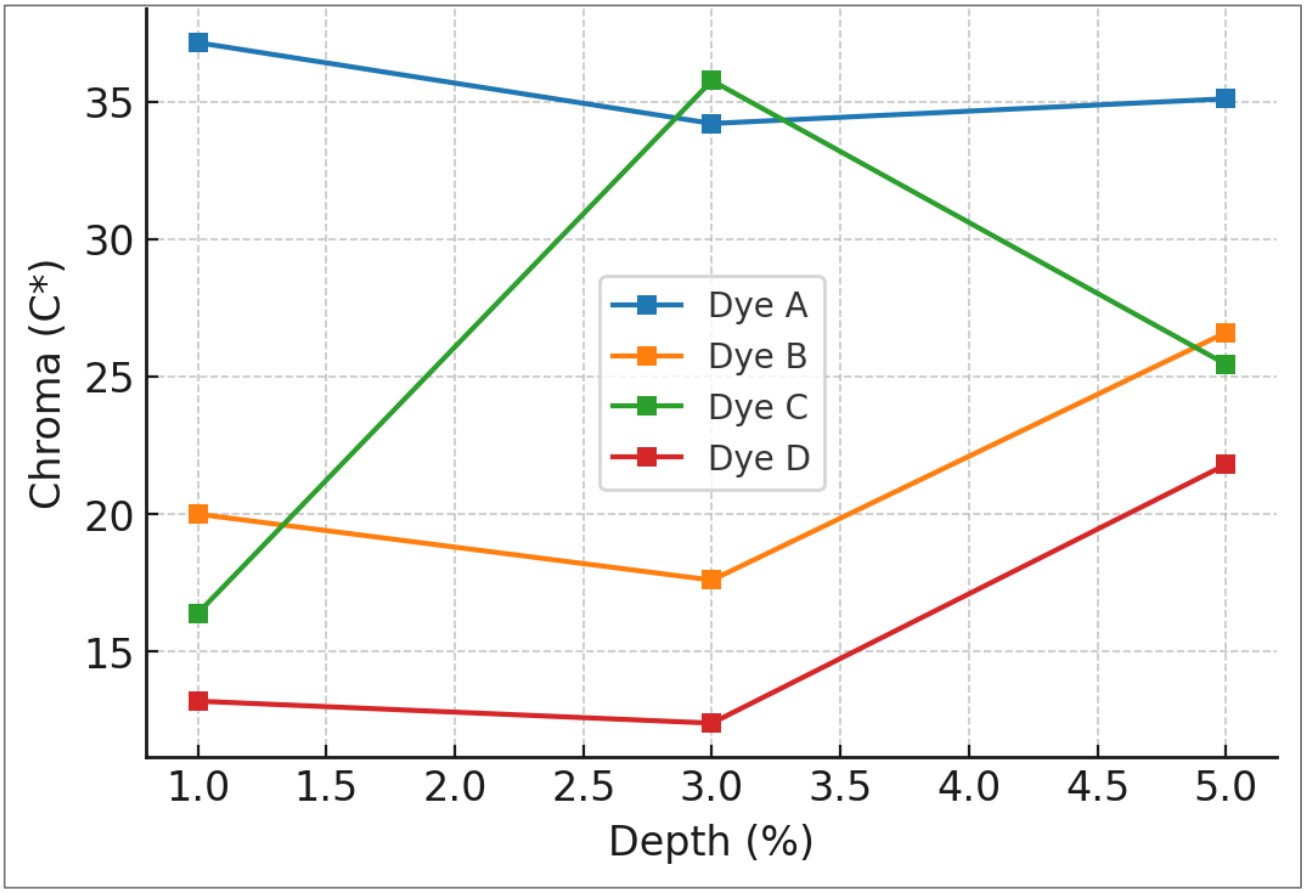

Figure 3: Chroma (C*) vs Depth on Nylon 6.6

Dyeing and Fastness Properties on Nylon 6.6 Fabrics

Dye Bath Exhaustion

The synthesized samples were dyed on the nylon 6.6 fabrics at a depth of 1 %, 3 % and 5 %. The results are presented in Table 5 and represented in Figure 2.

The exhaustion behavior of the synthesized dyes on nylon 6.6 is as given in Table 5 and represented graphically in Figure 2. Dye A had a consistently high uptake at all the concentrations used, with values varying between 90.2 ± 1.1% at the 1 % concentration, 94.0 ± 0.8%, 93.5 ± 1.2% at 3%, and 5% respectively. Such high uptake may be explained by the fact that the dye has high tinctorial strength and structural characteristics that contribute to resonance stabilization and high affinity to the fiber (Benkhaya *et al.*, 2020). Dye B also possessed an excellent exhaustion profile with uptake of 88.3 ± 0.9 at 1%, 90.4 ± 1.3 at 5%. This tendency can be attributed to the fact that the chromophore stabilization and moderate solubility make its appearance facilitated by the presence of one sulfonic acid functional group (Aspland, 1997).

In contrast, Dye C had a less consistent exhaustion profile. At the lowest dose of 1%, the exhaustion was minimal (56.7 ± 2.2%), and this increased steeply at higher concentrations to over 95 % at 5 %. This implies that, at the lower dye concentrations, accessibility and binding are limited, probably due to the reduction in the number of dye-fiber interactions and the consequent reduced resonance stabilization. However, at very high

concentrations, the interactions between dye and fiber are increased, and this observation is consistent with previous studies on acid dyes in polyamides (Siddiqua *et al.*, 2017).

Dye D had an intermediate affinity but an exhaustion of 72.5 ± 1.5 at 1%, greater than the exhaustion of Dye C at the same concentration. Its uptake however, rose proportionately with the concentration and was 89.7 ± 1.4% at 5%. Dye D does not seem to bind to fibers well, despite the two sulfonic acid functional groups, which would have allowed better solubility, probably because the chromophore resonance stabilization is reduced as reported in related systems (Eltaboni *et al.*, 2022).

The findings indicate that both solubilizing and structural functionalities contribute to a large extent to the efficiency of the dye exhaustion onto nylon 6.6. The different patterns of exhaustion observed with the various dyes serve as evidence of the role of the molecular structure of the dyes, especially the substitution pattern on the chromophore. These results are comparable with those of other researchers who indicate that the substitution pattern strongly influences the uptake of the naphthalimide-based azo dyes depending on dye-fiber interactions (Bekhanya *et al.*, 2020). The high values of exhaustion, especially that of Dye A and Dye C at high concentration points, clearly indicate their excellent performance in terms of their ability to stain compared to other reported naphthalimide derivatives, especially when directed to polyamide fibers.

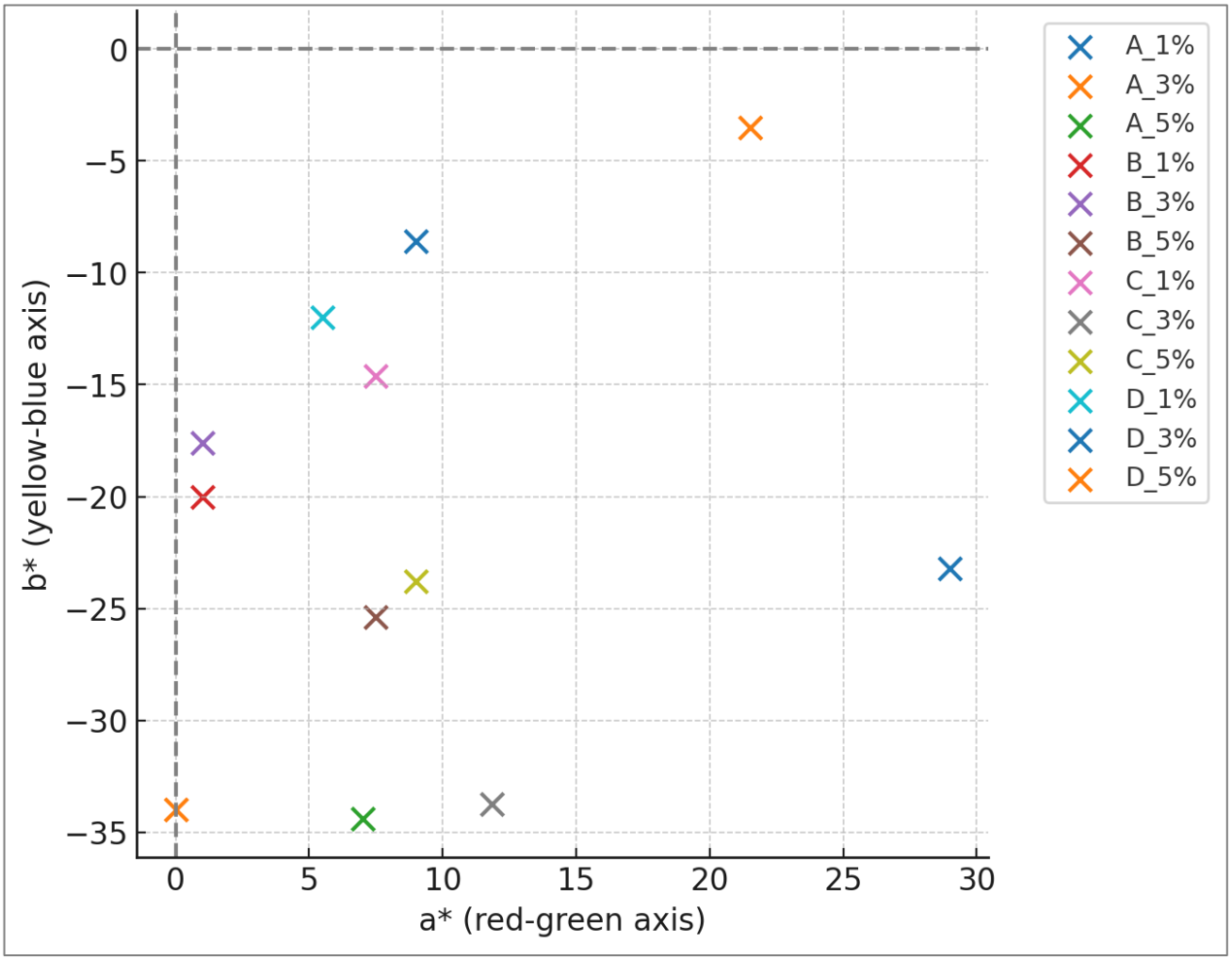

Figure 4: CIE a*–b* Coordinates of Dyed Nylon 6.6 Fabrics

Fastness Properties

The fastness characteristics of the synthesized naphthalimide-based azo dyes on nylon 6.6 are tabulated in Table 6. The dyes exhibited good to excellent performance across wash, perspiration, and light fastness tests, and the variability of replicates was also small, which evidences the reproducibility and accuracy of data.

Key words for fastness to wash and perspiration

1- Very poor; 2- fair; 3- good; 4- very good; 5- excellent

Key words for light fastness

8-Outstanding; 7-Excellent; 6-Very good; 5-Good; 4-Moderate; 3-Fair; 2-Poor; 1-Very poor

Wash fastness (color change) was classed generally between good and very good, with values achieved from 3.00 ± 0.00 to 4.50 ± 0.50. Dyes A and C were the most stable, with slightly higher fastness values and no change with dye depth. For example, Dye A was recorded to have values of 3.33 ± 0.33 and 4.00 ± 0.00 at 1 and 5 percent levels, whereas Dye C had 3.50 ± 0.50 and 4.50 ± 0.50

under similar conditions. Dye B demonstrated a decrease in performance at 2.67 ± 0.33 at 1 percent, while it increased to 3.33 ± 0.33 at 5 percent. This trend indicates that Dye B attaches better to the fiber when applied in higher concentrations, where a larger dye availability results in improved dye-nylon interactions.

Staining Fastness values were high irrespective of the dye used and were averagely 4.00 ± 0.00 implying minimal dye migration or bleeding. This indicates the high substantivity of these dye structures with nylon 6.6 and Dye B at 1%, although they did not exhibit good wash fastness. However, they showed good stain resistance, especially due to the strong adhesion of the dye to the fiber.

Perspiration Fastness had a greater variation at acidic and alkaline conditions. Acidic conditions resulted in lower values e.g. Dye C at 1% depth: 3.00 ± 0.00, whereas alkaline conditions were more resistant, with values going up to 5.00 ± 0.00 with higher depths. This performance observed in alkaline environments is in correlation with the increased ionic interactions of the sulfonated structures of dyes with the protonated nitrogen atoms of nylon in alkaline environments, as described by Aspland (1997).

Light Fastness values varied between 4.00 ± 0.00 (moderate) and 7.00 ± 0.00 (excellent), with the highest overall score being Dye C at 6.00 ± 0.00 to 7.00 ± 0.00 at 1 and 5 percent, respectively. An excellent light-fastness performance may also be explained by the peculiar structure of Dye C that promotes the resonance delocalization and minimizes the vulnerability to photobleaching (Christie, 2015). By comparison, Dye D also exhibited less light fastness (4.00 ± 0.00 to 5.00 ± 0.00), possibly due to its lower molar absorptivity and weaker resonance stabilization, leading to diminished photostability, particularly at higher depths. The increase in dye depth generally led to enhanced light fastness for all dyes, which is consistent with the well-established understanding that higher dye concentrations can reduce photoreactivity by increasing absorbance and limiting light penetration (Waring & Hallas, 2013).

The results underline the key importance of solubilizing substituents as well as resonance-stabilizing groups in determining the fastness of dyes. While all of the dyes exhibited good performance on nylon 6.6, Dye C was the most photostable, which resulted in excellent light fastness due to its strong resonance stabilization. Dye D lagged behind because of weaker electronic stabilization. These results indicate that a careful balance of substituents in naphthalimide azo dye systems can maximize dye uptake, wash and perspiration resistance, and long-term light fastness, classifying Dye C as particularly valuable where high light stability is demanded. Compared to most commercial acid dyes, especially milling and metal complex acid dyes applied to nylon 6,6, which mostly exhibit low wash fastness without after-treatment and which in many cases need syntan or the like to improve durability (Akyol Yılmaz and Becerir, 2022; Shokrzadeh *et al.*, 2025), the dyes presented here show marked improvement. Moreover, although acid dyes have poor to moderate wash fastness and light fastness ratings (usually between 3 and 5 on polyamide substrates) (Musa *et al.*, 2013), Dye C in the current study exhibited wash fastness up to 4.50 + 0.50 and outstanding light fastness (6.00 to 7.00). The above findings suggest that the structural variations of our naphthalimide-based dyes, particularly Dye C, facilitate increased dye-fiber interactions and result in considerably enhanced photostability as compared to those of standard commercial acid dyes.

Colour Assessment

The CIE coordinates of the synthesized naphthalimide-based azo dyes for 1%, 3% and 5% depth are presented in Table 7, the chroma vs depth plot is shown in Figure 3 and the digital swatches of the dyed fabrics is shown in Table 8. For the dyed nylon 6.6 fabrics, the positive a* values indicate a shift toward red tones, while the negative b* values indicate a shift toward blue tones. The chroma value is denoted as "C*" which denotes colour intensity or saturation, while the hue angle (ho) indicates the colour type.

Application of the CIE Lab system and the derived colourimetric coordinates (C, ho) provides a reliable indication of the visual characteristics of the dyed nylon 6.6 fabrics. In general, among all the dyes, there were significant changes in hue, chroma, and lightness as the depth increased, indicating structural variations and the concentration of dyes that impact the shade characteristics. The most dramatic shift of hue with depth levels was shown by dye A. When the depth was set to 1%, the shade was purple-violet (h^o = 321.7, C * = 37.14), however with the increase of the depth to 3 and 5 percent, a change was observed in the tone, becoming blue (270.0), blue-violet (281.5), respectively, and the lightness decreased (L * = 17.41 to 13.45). This implies good bath penetration and an enhancement of conjugated charge delocalization with shade buildup. As visualized in Figure 4, this marked hue progression indicates strong bath penetration and a high potential for depth-dependent shade tuning.

Dye B had lower chroma values (C* = 20.0-26.6) and fairly consistent blue-purple to violet hues at different depths (h^o = 272.9-286.5). The colors were more saturated and less chromatic (color shift) than the Dye A. This stability may be associated with the molecular structure of Dye B, or with a decrease in auxochromic interactions. Dye C, on the other hand, resulted in moderate chromatic colors that ranged from blue-violet to violet-magenta as concentration increased. The chroma was at a maximum of 35.76 with hue angle decreasing from 296.3° at 1% (purple) to 290.7° at 5%. The fairly constant chroma development indicates good solubility and balanced fiber affinity for Dye C.

Dye D imparted the brightest hues with the greatest lightness values (L = 63.5-73.4) and only slight differences in hue and L values among depth levels. The hue changed from purple-pink (h^o = 294.9°) to pink-magenta (ho = 350.8°) with a relatively large increase in a* values (21.5 at

5%), and a relatively low b* (-3.5). This pinkish inclination, combined with stable lightness values, indicates that dye D produces vibrant and vivid color hues. The measured changes in chroma and hue angle with dye depth are in agreement with the literature, where the distribution of electrons, substituent effect, and dye-fibre interaction have been associated with the visual perception of colour (Shore, 2002). This tunability is crucial in the development of fibre-specific dyes to meet market demands in terms of both functionality and aesthetics.

Table 8: Digital swatches of nylon 6.6 fabrics dyed with the synthesized naphthalimide-based azo dyes

DYES	1% SHADE	3% SHADE	5% SHADE
A			
B			
C			
D			

CONCLUSION

In this study, four new naphthalimide-based monoazo acid dyes were successfully synthesized, characterized, and used on nylon 6.6 substrates. Spectroscopic characterization and dyeing experiments confirmed the spectral purity, chromophoric efficiency, and integrity of each dye. In terms of chromometric analysis, combinations of CIELAB and CIE chromatic coordinates showed that the dyes produce an intense level and substrate-specific color that varies from purple-violet to pink-magenta with increasing chroma and hue variations at deeper levels. This was further indicated by good to excellent results from fastness testing, which showed good resistance to washing, perspiration, and light, all of which are major requirements for commercial viability. Structural parameters such as sulfonic acid location, conjugated π-systems, and positions of functional groups were found to be dominating in determining the dye fiber affinity and penetration behaviour, along with fastness properties. Although no empirical study was conducted on the environmental impact of these dyes, the rate of efficiency and fixations reported here encourages the potential for lower effluent load in practice. Additionally, a study of dyes on other fiber types and an assessment of the environmental impact of current dyes are also planned for future research. Overall, the results indicate the usefulness of naphthalimide as a general scaffold for the development of high-performance acid dyes for synthetic textiles by demonstrating the fine-tuning of its structure to modern dyeing requirements.

REFERENCES

AATCC. (2019). AATCC Test Method 61-2019: Colorfastness to laundering: Accelerated [Standard method]. American Association of Textile Chemists and Colorists.

AATCC. (2013). AATCC Test Method 15-2013: Colorfastness to perspiration [Standard method]. American Association of Textile Chemists and Colorists.

AATCC. (2014). AATCC Test Method 16.3-2014: Colorfastness to light: Xenon-arc [Standard method]. American Association of Textile Chemists and Colorists.

Akyol Yılmaz, G. and Becerir, B. (2022). Investigation of mordant application in reactive dyeing of nylon fabrics. AATCC Journal of Research, 10(2), 110–129. [Crossref]

Al-Majidi, S. M. and Al-Khuzaie, M. G. (2019). Synthesis and characterization of new azo compounds linked to 1,8-naphthalimide and studying their ability as acid-base indicators. *Iraqi Journal of Science*, 60(11), 2341–2352. [Crossref]

Al-Tohamy, R., Ali, S. S., Li, F., Okasha, K. M., Mahmoud, Y. A., Elsamahy, T., Jiao, H., Fu, Y. and Sun, J. (2022). A critical review on the treatment of dye-containing wastewater: Ecotoxicological and health concerns of textile dyes and possible remediation approaches for environmental

safety. *Ecotoxicology and Environmental Safety*, 231, 113160. [Crossref]

Ameuru, U. S., Yakubu, M. K., Bello, K. A., Nkeonye, P. O. and Halimehjani, A. Z. (2018). Synthesis of disperse dyes derived from 4-amino-N-decyl-1, 8-naphthalimide and their dyeing properties on polyester fabrics. *Dyes and Pigments*, *157*, 190–197. [Crossref]

Aspland, J. R. (1997). *Textile dyeing and coloration* (2nd ed.). American Association of Textile Chemists and Colorists. AATCC, Research Triangle Park, NC.

Autofab. (2024). *Nylon 6/6: A comprehensive overview*. Autofab. [Link]

Benkhaya, S., M'rabet, S. and Harfi, A. E. (2020). Classifications, properties, recent synthesis and applications of azo dyes. *Heliyon*, *6*(1), e03271. [Crossref]

Burkinshaw, S. and Son, Y. (2005). A comparison of the colour strength and fastness to repeated washing of acid dyes on standard and deep dyeable nylon 6,6. *Dyes and Pigments*, *70*(2), 156–163. [Crossref]

CIE (1931). *Commission Internationale de l'Eclairage (CIE) 1931 color space*.

Cohen, J., Wyszecki, G. and Stiles, W. S. (1968). Color Science: concepts and methods, quantitative data and formulas. *The American Journal of Psychology*, *81*(1), 128. [Crossref]

Christie, R. M. (2015). *Colour chemistry* (2nd ed.). Royal Society of Chemistry.

Dai, Y., Huang, H., Gao, H., Zhu, K., Zhang, L., Li, H. and Zhang, X. (2025). Rational design of a 1,8-naphthalimide-based fluorescent probe and its application in liquid food detection of viscosity and living cells. *Journal of Molecular Structure*, *1340*, 142529. [Crossref]

Ding, L., Zhang, H., Chen, L., Wang, Z., Pei, L., Yang, Q. and Wang, J. (2024). Improved Dyeing Performance of Blue Disperse Dyes with N-Acetoxyethyl Groups in D5 Non-aqueous Media System. *Fibers and Polymers*, *25*(3), 1005–1014. [Crossref]

Dodangeh, M., Grabchev, I., Staneva, D. and Gharanjig, K. (2021). 1,8-Naphthalimide derivatives as dyes for textile and polymeric materials: a review. *Fibers and Polymers*, *22*(9), 2368–2379. [Crossref]

Elmaaty, T. A., Sofan, M., Ayad, S., Negm, E. and Elsisi, H. (2022). Novel synthesis of reactive disperse dyes for dyeing and antibacterial finishing of cotton fabric under $scCO_2$. *Journal of CO_2 Utilization*, *61*, 102053. [Crossref]

Elmaaty, T., El-Aziz, E., Ma, J., El-Taweel, F. and Okubayashi, S. (2015). Eco-Friendly disperse dyeing and functional finishing of nylon 6 using supercritical carbon dioxide. *Fibers*, *3*(3), 309–322. [Crossref]

El-Sayed, E., El-Aziz, E. A., Othman, H. and Hassabo, A. (2024). Azo dyes: Synthesis, Classification and Utilisation in Textile Industry. *Egyptian Journal of Chemistry*, *0*(0), 0. [Crossref]

Eltaboni, F., Bader, N., El-Kailany, R., Elsharif, N. and Ahmida, A. (2022). Chemistry and applications of azo dyes: A comprehensive review. *Journal of Chemical Reviews,* 4(4), 313–330. [Crossref]

Geraghty, C., Wynne, C., & Elmes, R. B. (2021). 1,8-Naphthalimide based fluorescent sensors for enzymes. *Coordination Chemistry Reviews*, *437*, 213713. [Crossref]

Gharanjig, K., Arami, M., Bahrami, H., Movassagh, B., Mahmoodi, N. M. and Rouhani, S. (2007). Synthesis, spectral properties and application of novel monoazo disperse dyes derived from N-ester-1,8-naphthalimide to polyester. *Dyes and Pigments*, *76*(3), 684–689. [Crossref]

Gudeika, D. (2020). A review of investigation on 4-substituted 1,8-naphthalimide derivatives. *Synthetic Metals*, *262*, 116328. [Crossref]

Hosseinnezhad, M., Khosravi, A. R., Gharanjig, K., & Moradian, S. (2017). The comparison of spectra and dyeing properties of new azonaphthalimide with analogues azobenzene dyes on natural and synthetic polymers. *Arabian Journal of Chemistry, 10*(Suppl. 1), S3284–S3291. [Crossref]

Hunger, K. (2007). Industrial dyes: Chemistry, properties, applications. John Wiley & Sons.

Hunt, R. (2004). *The reproduction of colour*. [Crossref]

Jeong, C., Ahmad, A., Schmitz, H. C. and Cao, H. (2022). Synthesis and investigation of Fderivatives of 1,8-nFaphthalimide with a red emission via an aromatic nucleophilic substitution reaction. *Journal of Fluorescence*, *32*(2), 427–433. [Crossref]

Kant, R. (2012). Textile dyeing industry: An environmental hazard. *Natural Science*, 4(1), 22–26. [Crossref]

Khanum, R., Ali, R. S., Rangaswamy, H., Kumar, S. S., Prashantha, A. and Jagadisha, A. (2023). Recent review on synthesis, spectral studies, versatile applications of azo dyes and its metal complexes. *Results in Chemistry*, *5*, 100890. [Crossref]

Kreß, K. C., Fischer, T., Stumpe, J., Frey, W., Raith, M., Beiraghi, O., Eichhorn, S. H., Tussetschläger, S. and Laschat, S. (2013). Influence of chromophore length and acceptor groups on the optical properties of rigidified merocyanine dyes. *ChemPlusChem*, *79*(2), 223–232. [Crossref]

Mello, M. L. S., Anjos, E. H. D., & De Campos Vidal, B. (2024). Usefulness of sulfonated azo dyes to evaluate macromolecularly oriented protein substrates. *Acta Histochemica,* 126(3), 152154. [Crossref]

Musa, H., Abdulmumini, A., Folashade, M. O., Usman, B., & Abba, H. (2013). Studies on the dyeing of wool and nylon fabrics with some acid dyes. IOSR Journal of Applied Chemistry, 5(1), 11–17. [Crossref]

Netzer, F., Mahmud-Ali, A., Manian, A. P., Stephen, T. and Pham, T. (2025). Effect of dye aggregation on the sorption behavior of anionic dyes onto cationized cellulose fibers. *Langmuir*. [Crossref]

Nie, W. and Hu, L. (2024). Design of 1,8-naphthalimide-based fluorescent functional molecules for biological application: A review. *ChemistrySelect*, *9*(3). [Crossref]

Papapetros, K., Sygellou, L., Anastasopoulos, C., Andrikopoulos, K. S., Bokias, G., & Voyiatzis, G. A. (2023). Spectroscopic Study of the Interaction of Reactive Dyes with Polymeric Cationic Modifiers of Cotton Fabrics. *Applied Sciences,* 13(9), 5530. [Crossref]

Patel, H. M. and Dixit, B. C. (2011). Synthesis, characterization and dyeing assessment of novel acid azo dyes and mordent acid azo dyes based on 2-hydroxy-4-methoxybenzophenone-5-sulfonic acid on wool and silk fabrics. *Journal of Saudi Chemical Society*, *18*(5), 507–512. [Crossref]

Patel, H. S. and Patel, N. B. (2023). Synthesis, characterization and dyeing properties of acid dyes on wool, silk and nylon fibers. *IOSR Journal of Applied Chemistry*, *16*(11), 1–5. [Crossref]

Pendo, U. S., Bello, K. A., Yakubu, M. K., Giwa, A., Ameuru, U. S., Harifi-Mood, A. R. and Halimehjani, A. Z. (2023). Synthesis of monoazo disperse dyes derived from N-(1-phthalimidyl)-naphthalimides and their dyeing properties on polyester fabrics. *Pigment & Resin Technology*, *53*(6), 999–1007. [Crossref]

Penthala, R., Heo, G., Kim, H., Lee, I. Y., Ko, E. H. and Son, Y. (2020). Synthesis of azo and anthraquinone dyes and dyeing of nylon-6,6 in supercritical carbon dioxide. *Journal of CO_2 Utilization*, *38*, 49–58. [Crossref]

Rápó, E. and Tonk, S. (2021). Factors affecting synthetic dye adsorption; desorption studies: A review of results from the last five years (2017–2021). *Molecules*, *26*(17), 5419. [Crossref]

Sanaullah, N. and Walczak, K. (2025). 1,8-Naphthalimide derivatives as the small molecules with multiapplications in chemistry and biology. *Organic & Biomolecular Chemistry*. [Crossref]

Shaki, H., Gharanjig, K., & Khosravi, A. (2015). Spectral, dyeing and antimicrobial properties of some monoazo naphthalimide dyes on polyamide. *Indian Journal of Fibre & Textile Research, 40*(4), 425–430.

Shokrzadeh, S., Razbin, M., Ghaheh, F. S., Amiri, M. J., & Aghajanzadeh, S. (2025). Optimizing the eco-friendly dyeing of wool and nylon fabrics with *Prangos ferulacea* (L.) Lindl using artificial intelligence. *Scientific Reports*, *15*, 13267. [Crossref]

Shore J. (2002). *Colorants and auxiliaries: Volume 1: Colorants* (2nd ed.). Society of Dyers and Colourists.

Siddiqua, U. H., Ali, S., Iqbal, M. and Hussain, T. (2017). Relationship between structure and dyeing properties of reactive dyes for cotton dyeing. *Journal of Molecular Liquids*, 241, 839–845. [Crossref]

Soleimanigorgani, A., & Taylor, J. (2005). Dyeing of nylon with reactive dyes. Part 2. The effect of changes in level of dye sulphonation on the dyeing of nylon with reactive dyes. *Dyes and Pigments,* 68(2–3), 119–127. [Crossref]

Stevens, C., Stephen, T., Manian, A. and Pham, T. (Eds.). (2023). *Handbook of natural colorants*. John Wiley & Sons. [Crossref]

Waring, D. R., & Hallas, G. (2013). *The chemistry and application of dyes*. Springer Science & Business Media.

Westland, S., Ripamonti, C. and Cheung, V. (2012). *Computational Colour Science using MATLAB®*. [Crossref]

Zhang, L., Song, Q., Wang, Y., Chen, R., Xia, Y., Wang, B., Jin, W., Wu, S., Chen, Z., Iqbal, A., Liu, C. and Zhang, Y. (2024). Solvent-free mechanochemical synthesis of azo dyes. *RSC Mechanochemistry*, *1*(5), 447–451. [Crossref]

Appendix A: UV-Vis Spectra of Dye A, Dye B, Dye C and Dye D

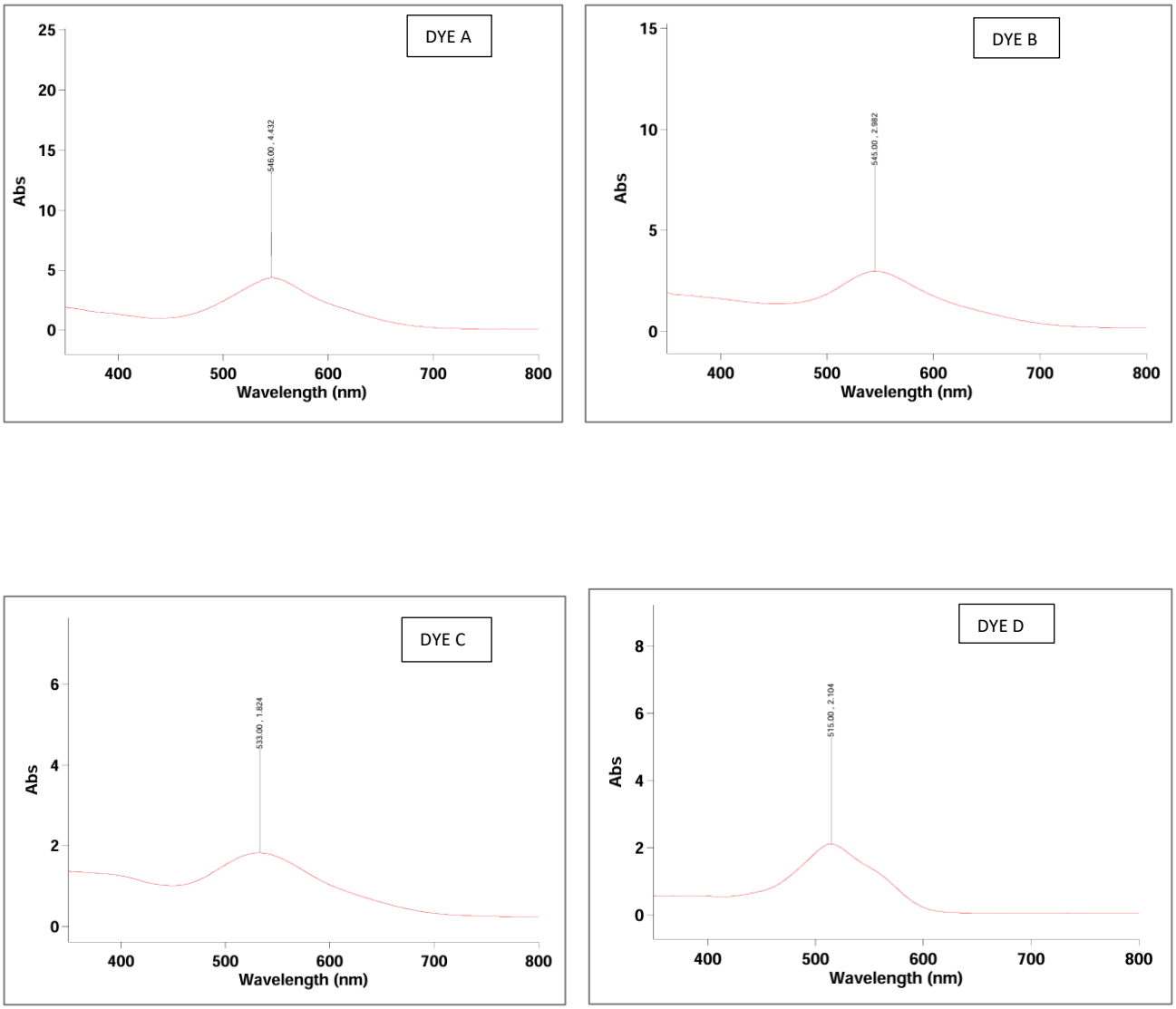

Appendix B: Mass Spectra of the Synthesized Intermediates and Dyes

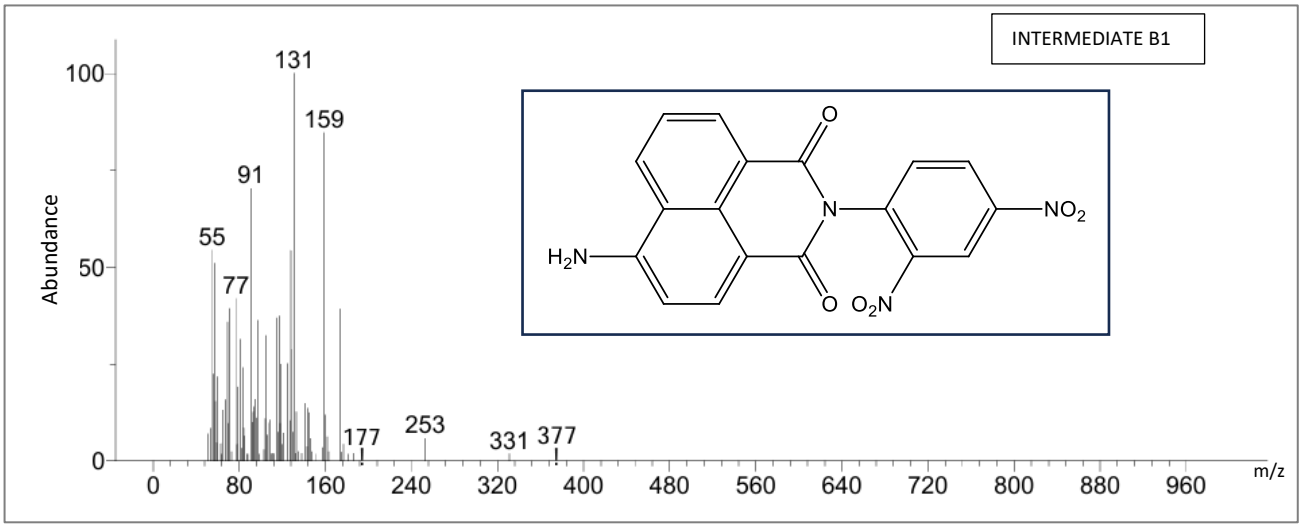

Figure B.1: MS for Intermediate B1

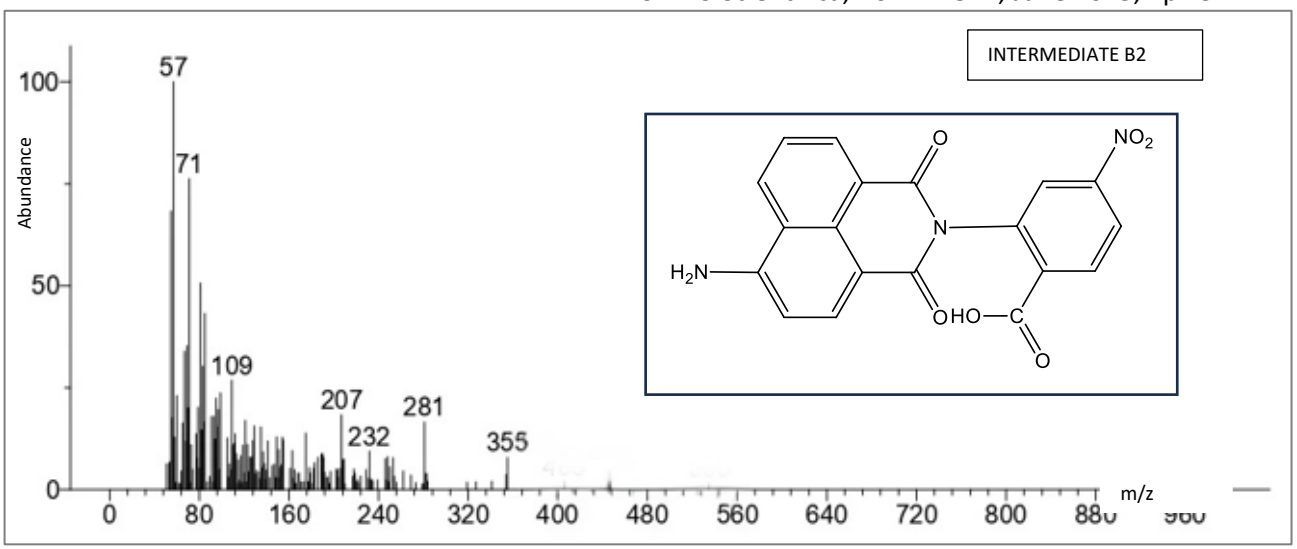

Figure B.2: MS for Intermediate B2

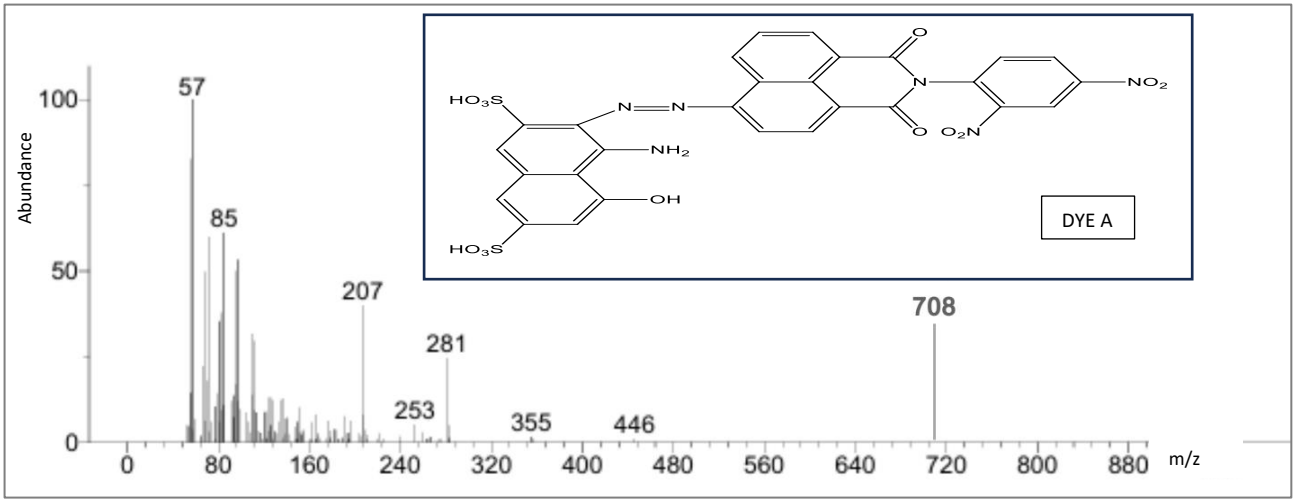

Figure B.3: MS for Dye A

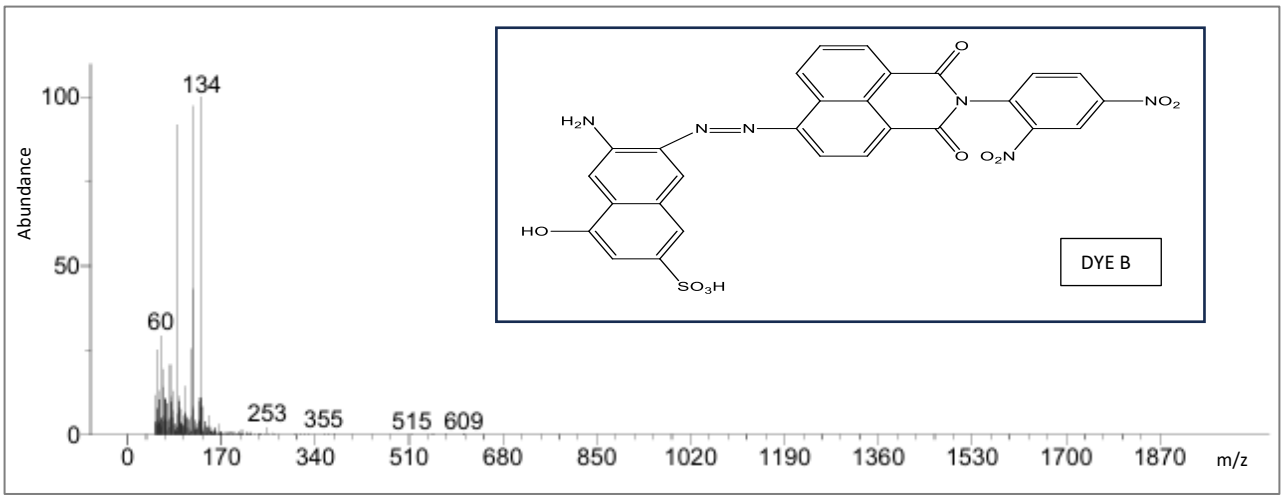

Figure B.4: MS for Dye B

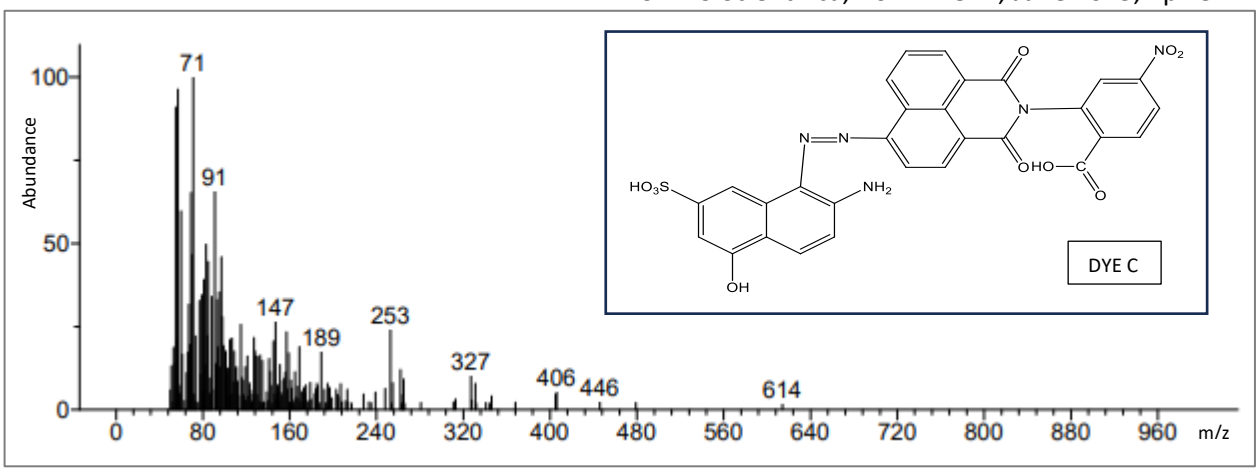

Figure B.5: MS for Dye C

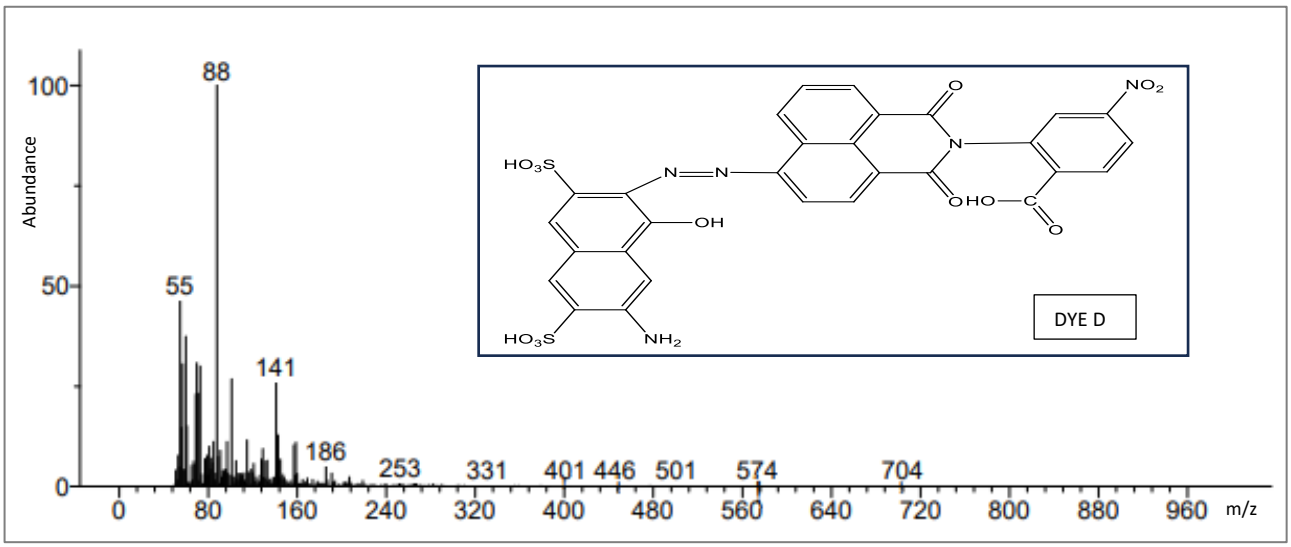

Figure B.6: MS for Dye D